Supporting Information

Three-dimension Cross-linked Co-MoS_2 Catalyst on Carbon Cloth for Efficient Hydrogen Evolution Reaction

Yan Xiao, Jing Yao, Tianze Zhang, Xinzhi Ma, Dexin Xu, and Hong Gao*.

School of Physics and Electronic Engineering, Key Laboratory for Photonic and Electronic Bandgap Materials, Ministry of Education, Harbin Normal University, Harbin 150025, People's Republic of China

*Corresponding author.

E-mail address: gaohong65cn@126.com

Chemicals. Thiourea (CH_4N_2S, Aladdin Chemistry Co., Ltd, AR), cobalt nitrate hexahydrate ($Co(NO_3)_2 \cdot 6H_2O$, Shanghai Macklin Biochemical Technology Co., Ltd, AR), urea (CH_4N_2O, Aladdin Chemistry Co., Ltd, AR), ammonium molybdate tetrahydrate ($(NH_4)_6Mo_7O_{24} \cdot 4H_2O$, Aladdin Chemistry Co., Ltd, ACS) and potassium hydroxide (KOH, Shanghai Macklin Biochemical Technology Co., Ltd, AR) were used directly without any further purification. The first-grade deionized (DI) water used in all experiments.

Synthesis of MoS_2/CC. For comparative studies, pure MoS_2 was synthesized to attain insights into the relationship between architecture and catalytic activity. Except without adding CoCH precursor, pure MoS_2 was prepared using a process similar to Co-MoS_2-4/CC.

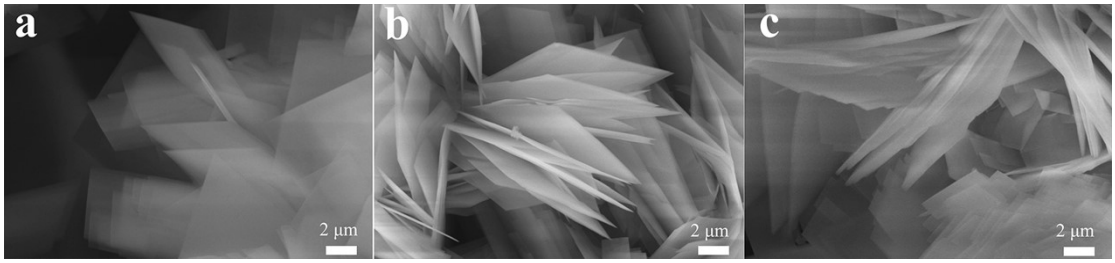

Figure S1. (a-c) High magnificent SEM images of CoCH-1/CC, CoCH-4/CC, and CoCH-8/CC, respectively.

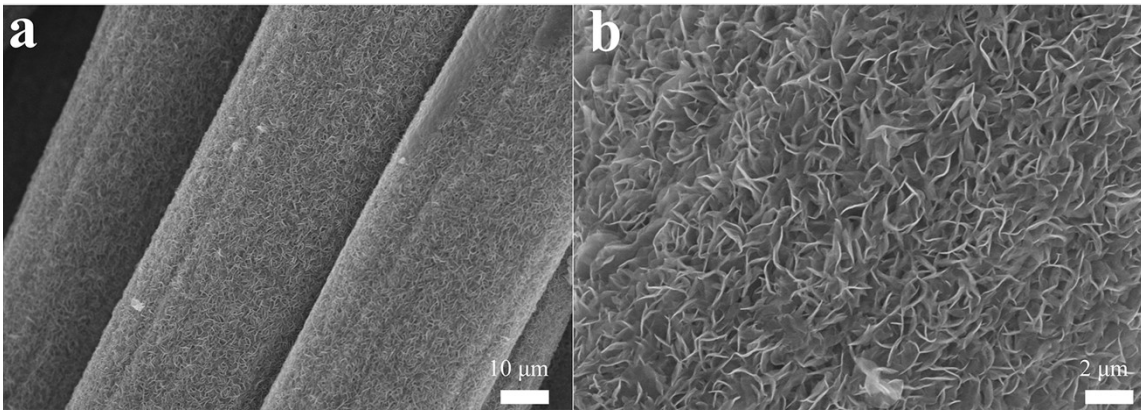

Figure S2. (a-b) Low and high magnificent SEM images of bare MoS_2.

a

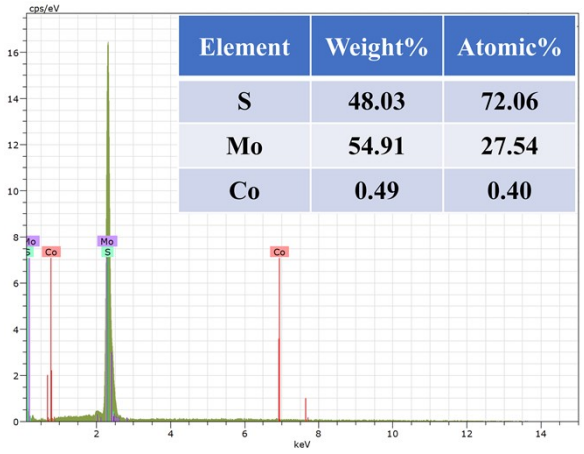

Element	Weight%	Atomic%
S	48.03	72.06
Mo	54.91	27.54
Co	0.49	0.40

b

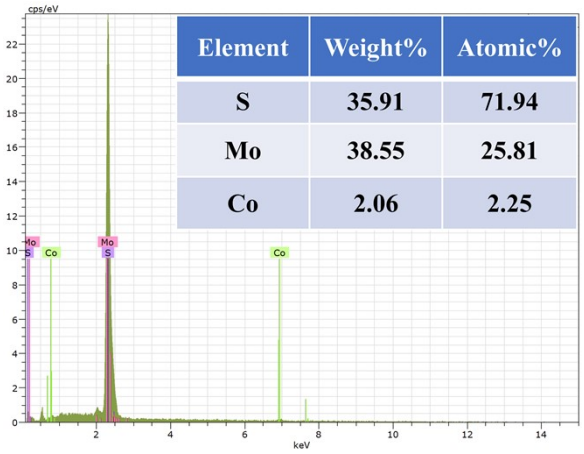

Element	Weight%	Atomic%
S	35.91	71.94
Mo	38.55	25.81
Co	2.06	2.25

c

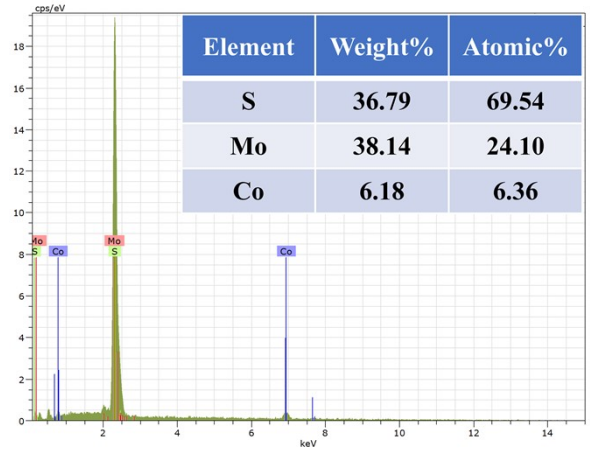

Element	Weight%	Atomic%
S	36.79	69.54
Mo	38.14	24.10
Co	6.18	6.36

Figure S3. (a-c) EDS data of Co-MoS_2-1, Co-MoS_2-4, and Co-MoS_2-8, respectively; insets show the corresponding stoichiometric ratios of S, Mo, and Co.

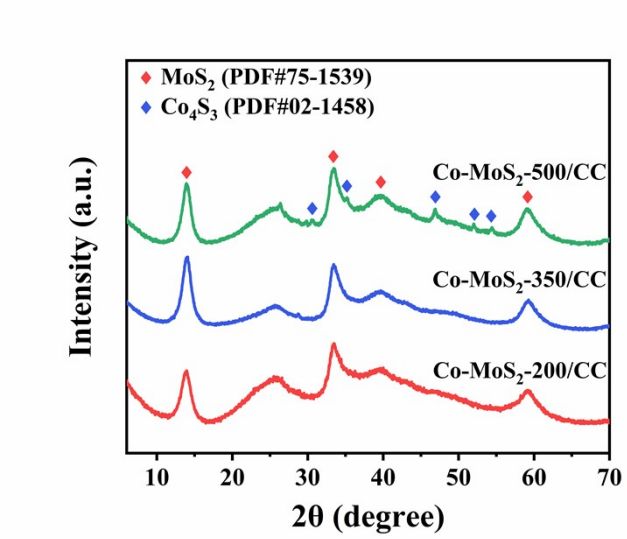

Figure S4. XRD patterns of the 3DSC Co-MoS_2-4/CC nanostructure synthesized at different reduction temperatures.

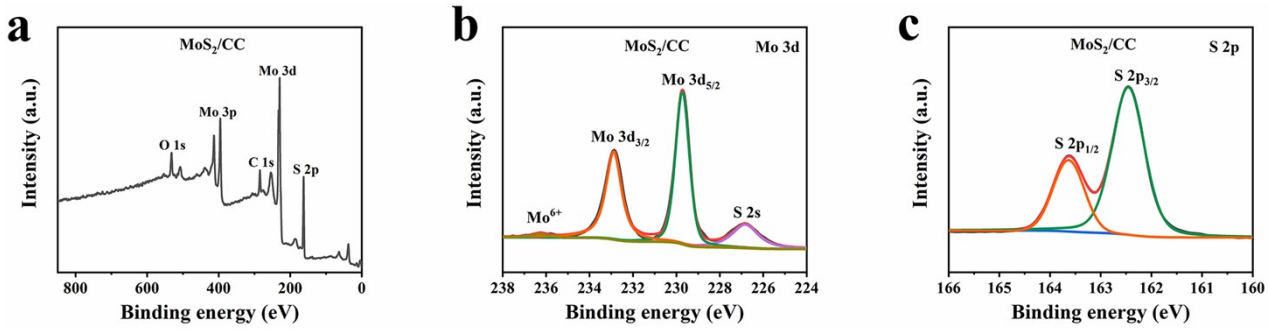

Figure S5. X-ray photoelectron spectroscopy (XPS) results of MoS_2/CC: (a) survey, (b) Mo 3d, and (c) S 2p regions.

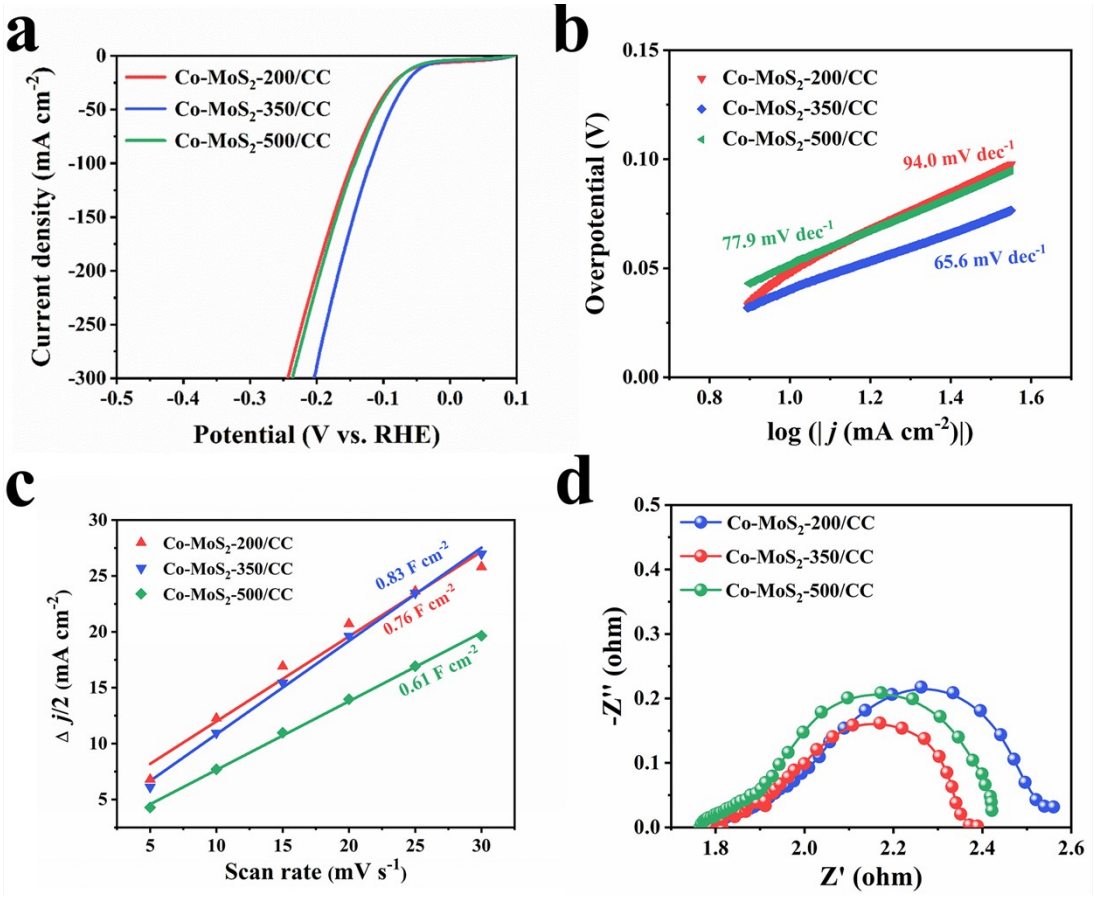

Figure S6. Comparison of HER activities of samples synthesized at changing annealing temperatures in 1 M KOH electrolyte. (a) The HER polarization curves and (b) Tafel plots for a series of Co-MoS_2-200/CC, Co-MoS_2-350/CC, and Co-MoS_2-500/CC electrocatalysts in 1 M KOH electrolyte. (c) Plots of $\Delta j/2$ versus scan rates. (d) Nyquist plots at an overpotential of 200 mV for electrodes.

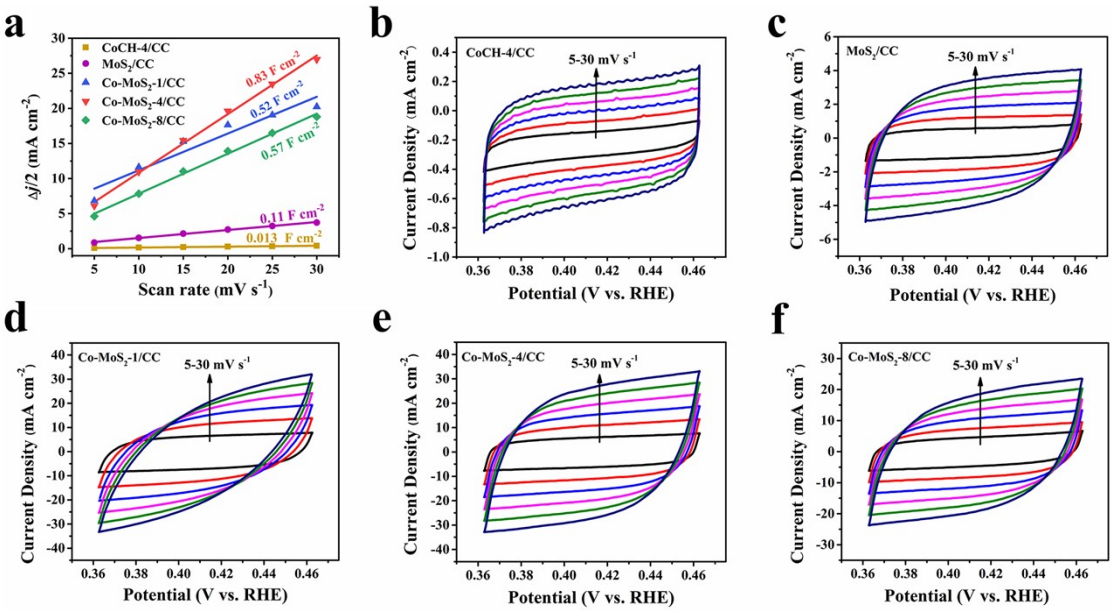

Figure S7. (a) Double layer capacitance estimated from the linear slope between Δj (= j_a - j_c) and scan rates. (b-f) CV curves at different scan rates for all synthesized catalysts.

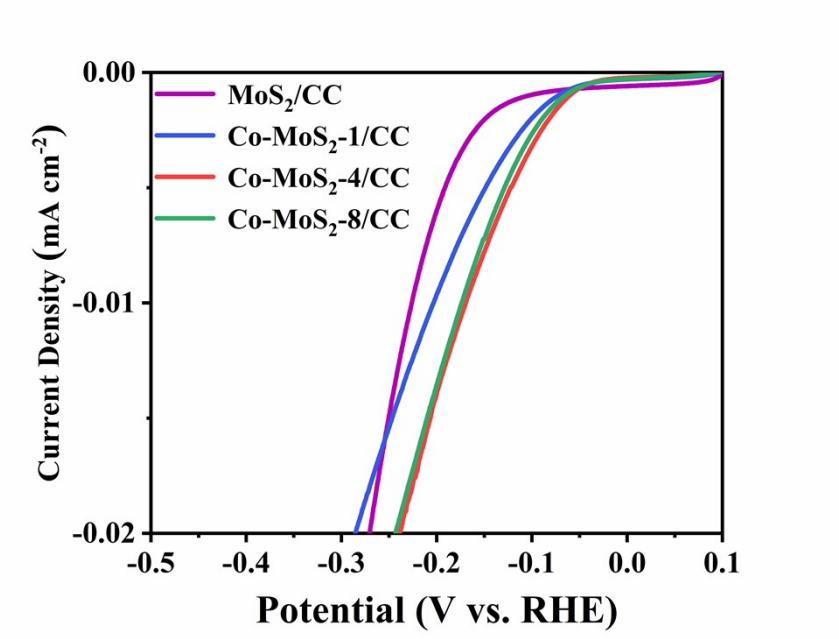

Figure S8. The final catalytic activity of a series of Co-MoS_2/CC electrodes after excluding the electrochemical surface area effects. Electrolyte: 1M KOH.

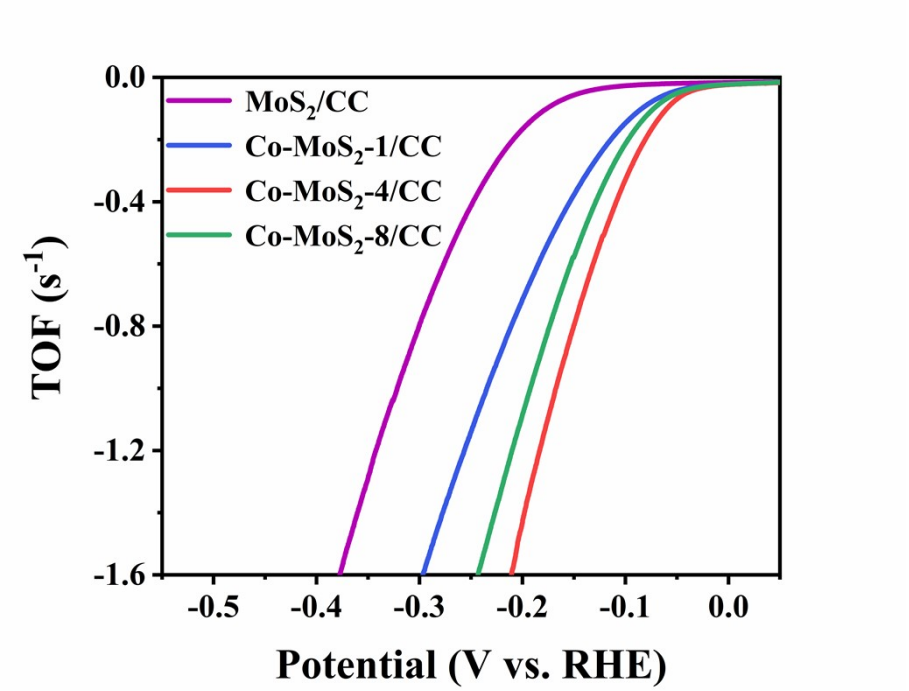

Figure S9. Potential-dependent TOF values of a series of Co-MoS_2/CC electrodes.

Table S1. Comparison of HER activity of Co-MoS_2-4/CC catalyst with other reported electrocatalysts in 1 M KOH electrolyte.

Catalyst	η_{10} (mV)	Reference
Co-MoS_2-4/CC	40	This Work
MoS_2/Ni_2O_3H	84	Small, 2020, 16, 2002212
Co_9S_8-MoS_2/NF	110	Adv. Funct. Mater., 30, 2020, 2002536
Ni/M-MoS_2	145	ChemElectroChem, 2020, 7, 3606-3615
1T-MoS_2/CoS_2	71	Small, 2020, 16, 2002850
MoS_2/CoS_2 NTs	85	J. Mater. Chem., A, 2019, 7, 13339-13346
1T-MoS_2 QS/$Ni(OH)_2$	57	Adv. Funct. Mater., 30, 2020, 2000551
MoS_2/FNS/FeNi	120	Adv. Mater., 30, 2018, 1803151
Co-Ni_3S_2-MoS_2/CA	89	Small, 2021, 17, 2006730
Co_3O_4/MoS_2	205	Appl. Catal. B-Environ., 2019, 248, 202-210
Co_4S_3/MoC-NSC-2	82.5	Appl. Catal. B-Environ., 2020, 260, 118197
N-NiS/NiS_2	185	Chem. Eng. J., 2020, 397, 125507
Ni_2P/Ni_3S_2	80	Nano Energy, 2018, 51, 26-36